

The Lagrangian Parcel Dynamics of Moist Symmetric Instability

KERRY A. EMANUEL

Department of Meteorology and Physical Oceanography, Massachusetts Institute of Technology, Cambridge 02139

(Manuscript received 18 February 1983, in final form 17 June 1983)

ABSTRACT

A simple model describing the slantwise ascent of a two-dimensional horizontal air tube subject to moist symmetric instability is developed under the assumptions that the Froude number is small and that mixing is absent. It is shown that, in general, the horizontal velocities attained by the tube are comparable to those of the mean flow and that vertical velocities of up to a few meters per second are possible. The tube ascends slantwise in such a way that its buoyancy remains nearly zero, unless the environment is very nearly moist adiabatic, in which case ascent at an angle of 45° to the vertical is preferred. Results of the analysis support the contentions of Bennetts and Hoskins and Emanuel that moist symmetric instability is the cause of some mesoscale rainbands. In a companion paper, it is demonstrated that the stability of the moist baroclinic atmosphere to two-dimensional slantwise displacements of arbitrary magnitude can be approximately assessed by reversibly lifting parcels along surfaces of constant angular momentum and comparing their density with that of their environment.

1. Introduction

A conspicuous and enigmatic feature of many extratropical cyclones is the presence of a multitude of banded features in the clouds and precipitation associated with the cyclones. These range from the mesoscale precipitation bands discussed by Browning and Harrold (1969), Houze *et al.* (1976), and many others to the somewhat more subtle phenomenon of multiple cloud layers east of the surface cyclone, as often seen by the observant air traveler. Not the least puzzling is the horizontal scale of the bands, which most often lies in a mesoscale range of from 50 to 500 km. In an attempt to explain these bands, it is natural to seek instabilities of larger scale flows which prefer these scales. Emanuel (1979) showed that, in addition to frontogenesis, symmetric instability is an instability which results in two-dimensional mesoscale motions; here "mesoscale" is taken to mean that the Rossby number of the flow is of order unity, and the Rossby number is defined as

$$Ro = \frac{\bar{V}_z H}{fL},$$

where \bar{V}_z is the vertical shear of the mean flow, H the depth of the unstable layer, f the Coriolis parameter, and L the horizontal scale of the motions resulting from the instability. Emanuel (1979) also suggested that symmetric instability may play a role in the formation of cloud and rain bands and squall lines, and Bennetts and Hoskins (1979; hereafter referred to as BH) demonstrate that the instability is likely to occur

in the moist baroclinic atmosphere, and suggested that frontal rainbands may result from such an instability. Motions resulting from this instability generally take the form of a series of slanted roll circulations, with axes along the mean geostrophic shear and with slopes in the vertical plane comparable to those of isentropic surfaces. A review of the classical theory of dry symmetric instability may be found in Emanuel (1979).

The addition of phase changes of water and the associated latent heating complicates the theoretical problem of symmetric instability immensely, in part since the effective stability of the atmosphere to vertical motions depends on the sign and magnitude of the vertical displacement. Despite the enormous increase in the complexity of the problem, one simplification occurs when the atmosphere is unstable only to upward displacements of sufficient magnitude: the resulting motions become largely localized in the vicinity of the clouds, and thus a first approximation to the convective dynamics can be obtained by assuming that the region outside the area where water is condensed and evaporated is unperturbed. The recognition of this simplification led originally to the "parcel dynamics" approach to moist convection, in which a moist parcel is assumed to ascend through and mix with its environment, the latter of which is taken to be otherwise unperturbed by the convection. An important assumption applied in parcel theory, which is directly related to the assumption of a stationary environment, is that perturbation pressure forces on the parcel may be neglected. A quantitative measure of the validity of this assumption is the

Froude number, which is broadly defined as the ratio of pressure gradient to body forces:

$$Fr \equiv \frac{|\alpha \nabla p|}{F_b},$$

where α is the specific volume, p the pressure, and F_b the sum of the body forces acting on a parcel. When the Froude number is small, the motion of the parcel can be estimated by assessing only the body forces (e.g., buoyancy) acting on the parcel. An *a posteriori* check on the smallness of the Froude number can be made by diagnosing the pressure field from the computed velocity field. We shall later show that the Froude number typical of moist symmetric instability will in general be somewhat smaller than that associated with moist convection.

Before proceeding, it is necessary to make a distinction between the type of moist symmetric instability considered by BH and the parcel instability examined here. In the former, the instability of an *entire fluid layer lifted to saturation* is examined; BH were able to show that the inviscid criterion for symmetric instability in cloudy air is the same as that for dry symmetric instability, but with the use of wet bulb potential temperature instead of potential temperature. Instead, we consider here the problem of *local conditional moist symmetric instability*, which results from the lifting of a spatially isolated small mass of air; the environment of such a parcel being considered to be unsaturated. I shall hereafter refer to this distinction as one between layer and parcel instability. The distinction is entirely analogous to the difference between convective and parcel instability as these terms are applied to the assessment of the susceptibility of the atmosphere to moist convection. In gen-

eral, layer instability is a necessary but insufficient condition for parcel instability. The parcel instability is generally regarded as being pertinent to the study of moist convection, since the environment of convective clouds is generally unsaturated. Whether this may also be true of moist symmetric instability, however, remains to be seen.

2. The parcel dynamics of moist symmetric instability

We consider a purely meridional, steady, moist baroclinic shear flow in thermal wind balance. By definition, the virtual potential temperature (θ_v) must in this case be a function of x and z only. Now consider the disposition of a small "tube" of air which extends indefinitely in the y direction and which is initially at rest at $z = 0$ (Fig. 1). We wish to examine the stability of this tube of air after it has been displaced a finite distance in an arbitrary direction in the x - z plane. In order to evaluate this stability, we initially neglect perturbation pressure forces which act on the moving tube, and also disregard the turbulent mixing of the air in the tube with its environment; the validity of these assumptions will be tested *a posteriori*.

Under these conditions, it is easily shown that a quantity M , where

$$M \equiv v + fx, \tag{1}$$

is conserved following the motion of the tube. This follows from the momentum equation in y in the absence of variations in y :

$$\frac{dM}{dt} = \frac{dv}{dt} + fu = 0.$$

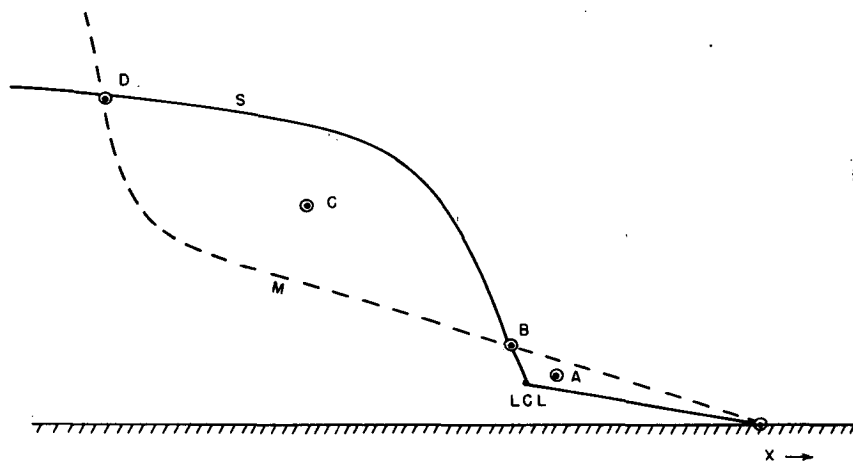


FIG. 1. Hypothetical configuration of M (dashed) and S (solid) surfaces as viewed in a plane which is orthogonal to the mean vertical shear vector. The S surface is defined with respect to the encircled surface tube. The position of this tube and point D are stable equilibrium positions for reversible displacements of the surface tube, while point B is an unstable equilibrium position. The tube, when reversibly displaced to A , will return to its initial position; if it is displaced to C it will accelerate toward D .

If the mean meridional flow increases upward, then M must increase upward and with x , according to (1). A possible surface along which M is constant and equal to the value of M in the air tube under consideration is illustrated by the dashed line in Fig. 1.

In general, the virtual potential temperature (θ_v) of the air tube will also be conserved unless phase changes of water occur, in which case θ_v may be considered to be a function of z alone, following the motion of the tube and neglecting the effect of horizontal variations of pressure on the saturation mixing ratio. We define a particular surface S in the x - z plane such that the θ_v of the air tube lifted reversibly along the surface is always equal to that of the environment. The x and z coordinates of such a surface may be obtained from the definition

$$\theta_v(x, z) = \theta_{vt}(x_0, z_0, z), \quad (2)$$

where the subscript t refers to the tube quantity, and x_0 and z_0 are the initial coordinates of the tube. It should be noted that S surfaces, unlike M surfaces, cannot be defined without reference to a particular sample of air. In the special case where the air tube is dry, $\theta_{vt} = \theta_t = \text{constant}$, and S surfaces correspond to θ surfaces. If the environment is everywhere saturated, S surfaces are equivalent to surfaces of constant equivalent potential temperature.

A possible configuration of such a surface, defined with respect to the θ_v of a surface air tube, is illustrated by the solid line in Fig. 1. Between the initial position of the tube and its lifted condensation level (LCL), the S surface is simply a surface of constant θ_v . Above the LCL, the S surface is neither a surface of constant θ_v nor one of constant θ_{e0} , but simply continues to represent the locus of points along which the tube's buoyancy vanishes.

Again neglecting mixing and perturbation pressure forces, we may write the equations of motion of the tube in x and z as

$$\frac{du}{dt} = f(v - v_g) = f(M_t - M_g), \quad (3)$$

$$\frac{dw}{dt} = \frac{g}{\theta_{v0}} (\theta_{vt} - \theta_{vg}), \quad (4)$$

where f is the Coriolis parameter (assumed constant), θ_{v0} is a constant reference virtual potential temperature, and the subscript g refers to the geostrophically balanced M and θ_v which constitute the unperturbed environment of the tube. The thermal wind relation requires that

$$f \frac{\partial M_g}{\partial z} = \frac{g}{\theta_{v0}} \frac{\partial \theta_{vg}}{\partial x}. \quad (5)$$

The expressions (3) and (4) simply show that the x and z accelerations experienced by the tube will be proportional to its M and θ_v surpluses, respectively. In reference to Figs. 1 and Eqs. (3) and (4), it is seen

that if the air tube initially at rest at $z = 0$ is displaced to point A, its M and θ_v will be greater than and less than those of its environment, respectively, and the net acceleration on the tube will act to return it to its initial position. By similar reasoning, a displacement to point C will result in an upward and westward unstable acceleration. Points B and D as well as the initial point are equilibrium positions of the air tube; point D and the initial point represent stable equilibria while point B is an unstable equilibrium position. Point B may be regarded as the "level of free slantwise convection (LFS)."

As an illustration of the motion of a tube as governed by (3) and (4), we examine a simple atmosphere in which, in a lower layer, v is a linear function of z and x , the air is saturated, and the lapse rate of the atmosphere is exactly moist adiabatic at a particular longitude $x = 0$. In an upper layer, above $z = H$, there is no vertical shear and the lapse rate is more stable than moist adiabatic. We examine the motion of a tube initially at rest at $x = z = 0$ with $M = M_t$ and $\theta_v = \theta_{vt}$. The configuration of M and S surfaces emanating from $x = z = 0$ is illustrated in Fig. 2. By definition, the M and θ_v surfaces in the lower layer obey

$$M_g = \bar{v}_z z + (f + \bar{v}_x)x = \bar{v}_z z + \bar{\eta}x, \quad (6)$$

$$\theta_{vg} = \theta_{vt}(z) + \frac{\theta_{v0}}{g} f \bar{v}_z x, \quad (7)$$

where \bar{v}_z and \bar{v}_x are the constant vertical and horizontal shears of \bar{v} , $\bar{\eta}$ is the mean absolute vorticity in the z direction, and the last term in (7) reflects the thermal wind balance (5). In the upper layer, the M surfaces are vertical while the S surfaces are horizontal, so that both the M and S surfaces have kinks at $z = H$, as shown in Fig. 2. Note that qualitatively, the tube has an unstable equilibrium at its initial position, and after motion begins, it will arrive at point 1 (Fig. 2) and oscillate around this new equilibrium point. The horizontal distance traversed between these equilibrium positions is

$$L = - \frac{\partial M / \partial z}{\partial M / \partial x} H = \frac{-\bar{v}_z}{\bar{\eta}} H. \quad (8)$$

Note that the Rossby number defined using this scale is close to 1. Since typically \bar{v}_z lies in the range 10 – 100η , L will be between 10 and $100H$.

The trajectory of the tube up until it reaches $z = H$ can be found by integrating (3) and (4). Substituting (6) and (7), we have

$$\frac{du}{dt} \equiv \frac{d^2x}{dt^2} = -f(\bar{v}_z z + \bar{\eta}x), \quad (9)$$

$$\frac{dw}{dt} \equiv \frac{d^2z}{dt^2} = -f\bar{v}_z x. \quad (10)$$

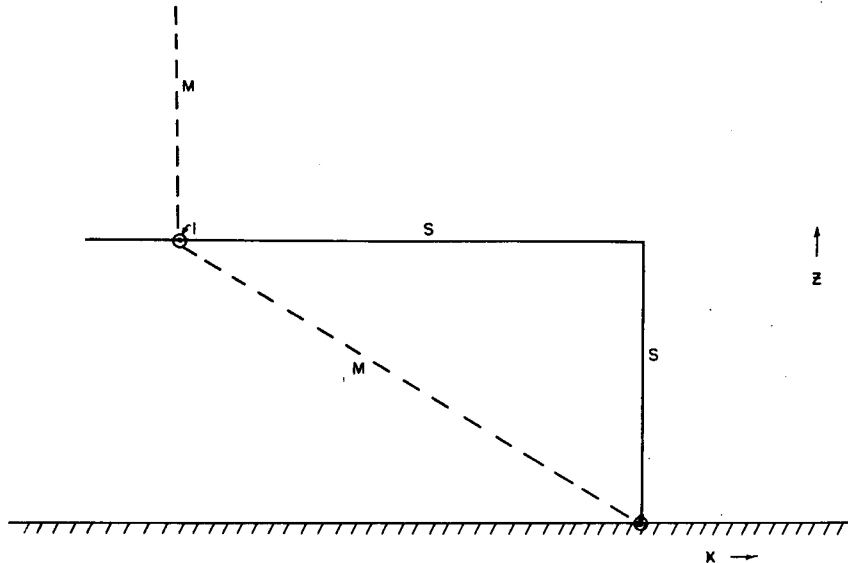


FIG. 2. Configuration of *M* (dashed) and *S* (solid) surfaces for the simple non-hydrostatic calculation of the Lagrangian motion of the surface tube. The stable equilibrium position of this tube is at point 1.

Differentiating (9) twice in time and substituting from (10) yields

$$\frac{d^4x}{dt^4} + f\bar{\eta} \frac{d^2x}{dt^2} - f^2\bar{v}_z^2x = 0. \tag{11}$$

Solutions of (11) will have the general form $\exp(\sigma_1 t)$, with

$$\sigma_1^2 = \frac{1}{2}f\bar{\eta}[-1 \pm (1 + 4\bar{v}_z^2\bar{\eta}^{-2})^{1/2}] \approx \pm f\bar{v}_z. \tag{12}$$

The approximation in (12) can be made when $\bar{v}_z \gg \bar{\eta}$, which is very well satisfied even in weak baroclinic flows. The general solution of (11) with specified initial conditions is

$$x = \frac{u_0 - w_0}{2\sigma} \sinh(\sigma t) + \frac{u_0 + w_0}{2\sigma} \sin(\sigma t), \tag{13}$$

$$z = \frac{w_0 - u_0}{2\sigma} \sinh(\sigma t) + \frac{u_0 + w_0}{2\sigma} \sin(\sigma t), \tag{14}$$

where u_0 and w_0 are the initial horizontal and vertical velocities, respectively, and the tube is assumed to lie initially at $x = z = 0$. Here we take

$$\sigma \equiv (f\bar{v}_z)^{1/2}. \tag{15}$$

It is clear from (13) and (14) that at large time, the tube accelerates upward in such a way that $x = -z$; i.e., at a 45° angle to the vertical. This will be true at all times provided that $u_0 = -w_0$, otherwise the tube will also execute an oscillation about the 45° trajectory. This trajectory, to a close approximation, lies halfway between the *M* and *S* surfaces. The velocities associated with the ascent are

$$u = \frac{1}{2}(u_0 - w_0) \cosh(\sigma t) + \frac{1}{2}(u_0 + w_0) \cos(\sigma t), \tag{16}$$

$$w = \frac{1}{2}(w_0 - u_0) \cosh(\sigma t) + \frac{1}{2}(u_0 + w_0) \cos(\sigma t). \tag{17}$$

In the limit of small u_0 and w_0 and large time, we may easily substitute x for t as the independent variable, from (13), whence we obtain

$$z = -x, \quad u = \sigma x, \quad w = -\sigma x. \tag{18}$$

By the time the tube reaches $z = H$, it will have an upward velocity of σH , which from (15), will usually be on the order of several meters per second.

In reference to Fig. 2, it is clear that after the tube reaches $z = H$, $x = -H$, it will begin to accelerate horizontally toward its new equilibrium position, while also executing an oscillation about the horizontal *S* surface. Ignoring this oscillation, we can restart the integration of (6) using

$$M_g = \bar{v}_z H + \bar{\eta} x,$$

with the initial conditions taken from (18):

$$x_0 = -H, \quad u_0 = -\sigma H,$$

and with w_0 set equal to zero by way of disregarding the vertical oscillation. The solution may be expressed with x as the independent variable:

$$u^2 = f[\bar{v}_z H(-H - 2x) + \bar{\eta}(H^2 - x^2)], \tag{19}$$

where for consistency u is taken to be negative. From the above, it is evident that the maximum velocity occurs at the equilibrium position, $x = -\bar{v}_z H/\bar{\eta}$, and again assuming that $\bar{v}_z \gg \bar{\eta}$, this velocity is nearly

equal to a $\bar{v}_z H(f/\bar{\eta})^{1/2}$. Thus the maximum velocity attained by the tube is comparable to the velocity of the mean flow. The maximum penetration of the tube will be at $x \approx -2\bar{v}_z H/\bar{\eta}$.

The most serious deficiency of this model is probably the neglect of turbulent mixing between the tube and its environment. While the velocities in the x - z plane are small during the ascent of the tube, very large differences between the meridional velocity of the tube and that of its environment develop. It seems very likely that waves will develop in the direction along the tube, destroying its initial symmetry. A transition to turbulence is quite likely to occur early in the tube's trajectory; the validity of the aforementioned solution beyond this point is thus highly questionable.

Another simple case which may be less prone to turbulence occurs when the M and S surfaces are flat planes (and the S surface is not vertical). Such will be the case when

$$M_g = M_t + \bar{v}_z z + \bar{\eta} x, \tag{20}$$

$$\theta_{vg} = \theta_{vt}(z) + N^2 z + f \bar{v}_z x, \tag{21}$$

where N is a constant which can be interpreted as the local buoyancy frequency of the tube. We again define an upper layer where $\bar{v}_z = 0$, so that both the M and S surfaces have kinks at $z = H$ (Fig. 3).

Substituting (20) and (21) into (3) and (4) yields

$$\frac{d^2 x}{dt^2} = -f(\bar{v}_z z + \bar{\eta} x), \tag{22}$$

$$\frac{d^2 z}{dt^2} = -N^2 z - f \bar{v}_z x. \tag{23}$$

If both the M and S surfaces have small slopes, then on the average, the vertical velocities and accelerations will be much less than their horizontal counterparts and the hydrostatic approximation can be

made. Thus we set (23) equal to zero, which also has the effect of eliminating oscillations in the system. Then

$$z = -f \bar{v}_z x / N^2, \tag{24}$$

$$\frac{d^2 x}{dt^2} = f^2 (\bar{v}_z^2 / N^2 - \bar{\eta} / f) x \equiv \sigma^2 x. \tag{25}$$

The solution of (25) can be expressed in terms of x as the independent variable. In the limit of vanishing initial velocity, we have

$$u = \sigma x, \quad w = -f \bar{v}_z u / N^2. \tag{26}$$

The solutions (24) and (26) describe the tube's ascent which, in the hydrostatic limit, is directly along an S surface. When the tube reaches $z = H$, its horizontal velocity will be

$$u = -v_0 \text{Ri} \left(\frac{1}{\text{Ri}} - \bar{\eta} / f \right)^{1/2}, \tag{27}$$

where $v_0 \equiv \bar{v}_z H$ and $\text{Ri} \equiv N^2 / \bar{v}_z^2$.

Following the same procedure as in the moist adiabatic case, we can find the zonal velocity of the tube after it reaches $z = H$; it is the negative root of

$$u^2 = -[2f \bar{v}_0 x + f \bar{\eta} x^2] - v_0^2 \text{Ri}. \tag{28}$$

We find that the maximum velocity achieved by the tube is $v_0(f/\bar{\eta} - \text{Ri})^{1/2}$, which occurs at $x = -v_0/\bar{\eta}$. The maximum zonal penetration of the tube in this case is

$$x_{\text{max}} = -v_0 \bar{\eta}^{-1} [1 + (1 - \bar{\eta} / f \text{Ri})^{1/2}].$$

The tube again reaches a new equilibrium after having traversed a horizontal distance which makes the Rossby number 1. Since the tubes follow S surfaces they have no buoyancy, and since the flow in this case is statically stable, the local Richardson number in the vicinity of the tubes may not be so small that turbulence sets in. In particular, the maximum zonal

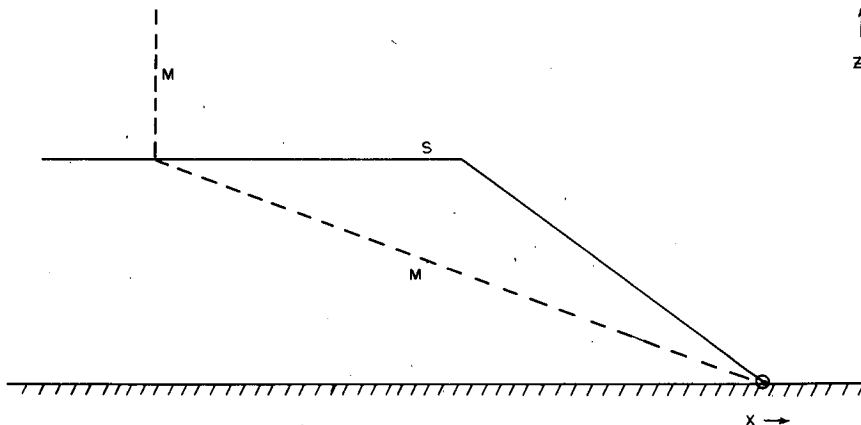


FIG. 3. As in Fig. 2, but for the hydrostatic case.

velocity achieved by the tube, and the maximum difference between the tube's meridional velocity and that of its environment are, respectively,

$$u_{\max} = v_0(f/\bar{\eta} - \text{Ri})^{1/2},$$

$$|M_t - M_{en}|_{\max} = v_0(1 - \bar{\eta} \text{Ri}/f).$$

The condition that $\text{Ri} = f/\bar{\eta}$ is just the condition that the S and M surfaces coincide, and this is in turn the marginal state for instability. If the flow is only weakly unstable, and provided that the slantwise ascending motion is not too narrowly confined, the flow may remain laminar. When the conditions are more supercritical, turbulence is likely since the velocities within the comparatively narrow ascending region will be comparable to those of the mean flow.

By contrast to the assumption of adiabatic ascent, the small Froude number approximation applies very well in this problem, as a consequence of the large aspect ratio of the drafts which result. This can be demonstrated by diagnosing the perturbation pressure and thereby determining the order of magnitude of the perturbation pressure gradient acceleration. Taking the divergence of the Boussinesq form of the inviscid primitive equations in two dimensions, we obtain

$$\bar{\alpha} \nabla^2 p' = f \frac{\partial v'}{\partial x} + \frac{\partial B'}{\partial z} + \left(\frac{\partial u}{\partial x}\right)^2 + \left(\frac{\partial w}{\partial z}\right)^2 + 2 \frac{\partial w}{\partial x} \frac{\partial u}{\partial z},$$

where $\bar{\alpha}$ is a reference specific volume, and primes refer to departures from geostrophic and hydrostatic equilibrium. Referring to Fig. 4, we make the following estimates of the magnitudes of each term in the above expression:

$$\bar{\alpha} \nabla^2 p' \approx \frac{p'}{d^2} + \frac{p'}{L_s^2} \sim \frac{p'}{d^2},$$

$$f \frac{\partial v'}{\partial x} \approx f \frac{v'}{L} = f \frac{v'}{d} \sin \theta,$$

$$B' \approx 0 \text{ (hydrostatic),}$$

$$\left(\frac{\partial u}{\partial x}\right)^2 = \left(\frac{\partial w}{\partial z}\right)^2 \approx \frac{\partial w}{\partial x} \frac{\partial u}{\partial z} \approx \frac{u^2}{L^2} = \frac{u^2}{d^2} \sin^2 \theta.$$

Using these estimates, we estimate the Froude number for horizontal accelerations as

$$\text{Fr}_x \equiv \frac{\bar{\alpha} \partial p' / \partial x}{f v'} \approx \sin^2 \theta \left(1 + \frac{u^2}{f v' d} \sin \theta \right).$$

Taking the liberal estimates $u' \approx v' \approx v_0$ and using $\sin \theta \approx f \bar{v}_z / N^2$,

$$\text{Fr}_x \approx \sin^2 \theta \left(1 + \frac{H}{d} \frac{1}{\text{Ri}} \right)$$

Provided, then, that $d \gg \text{Ri}^{-1} H \sin^2 \theta$, the effective Froude number will be very small in the hydrostatic case; this is effectively a consequence of the large aspect ratio of the draft.

Boundaries and the finite convergence of mass into the ascending moist flow may have important consequences on the further development of the instability. Fig. 5 illustrates the qualitative nature of the two-dimensional finite mass circulation resulting from conditional symmetric instability, following the present work, that of BH, and Emanuel (1982). The major effects of the part of the flow which advects temperature and moisture will be to cause a local overturning of θ_e surfaces and concomitant moist convection, as shown by BH, and also, possibly, a frontogenetical circulation due to the deformation in the x - z plane. The direct effect of the advection of equivalent potential temperature upon the instability may be understood by expressing the Lagrangian growth rate of the hydrostatic disturbance (25) in terms of the equivalent potential vorticity, defined as

$$q_e \equiv (f \mathbf{k} + \nabla \times \mathbf{v}) \cdot \nabla \ln \theta_e, \tag{29}$$

where θ_e is the equivalent potential temperature, \mathbf{v} the velocity vector, and \mathbf{k} the unit vertical vector. If *both the environment and the tube are saturated*, then the buoyancy frequency N , which appears in (25), is the saturated frequency N_w . As shown by Durran and Klemp (1982), this may be expressed as

$$N_w^2 = g \frac{\Gamma_m}{\Gamma_d} \frac{\partial}{\partial z} \ln \theta_e,$$

where Γ_m and Γ_d are the moist and dry adiabatic lapse rates, respectively, and we have neglected small terms which depend on the total water content. It may also be shown that the thermal wind relation, to the same degree of approximation, takes the form

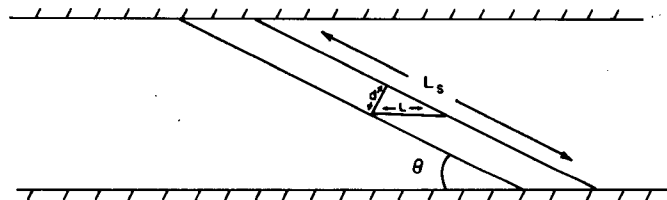


FIG. 4. Schematic geometry of a slantwise updraft. L_s is the length along the draft, while d is its width. The draft has slope $\tan \theta$, and the horizontal distance across the draft is L .

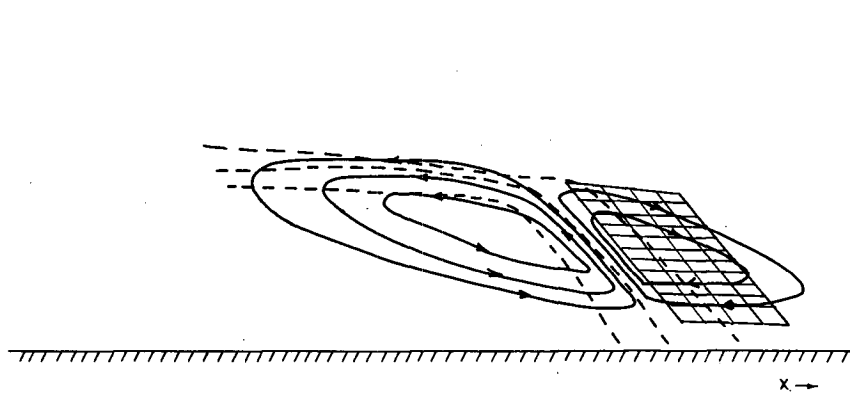


FIG. 5. Estimated mass circulation resulting from moist symmetric instability. The dashed lines show position of base-state θ_e surfaces, and the shading denotes the region in which these surfaces are being overturned by the circulations. By Eq. (31), the Lagrangian growth rate will increase in this region.

$$f\bar{v}_z = g \frac{\Gamma_m}{\Gamma_d} \frac{\partial}{\partial x} \ln \theta_e. \quad (30)$$

With these two expressions and (29), the Lagrangian growth rate (25) may be written

$$\sigma^2 = -fq_e \left(\frac{\partial \ln \theta_e}{\partial z} \right)^{-1}. \quad (31)$$

Thus, as noted by BH, the equivalent potential vorticity must be negative for conditional symmetric instability in a convectively stable atmosphere.¹ Here we find that the Lagrangian growth rate increases as the lapse rate of θ_e decreases; when the latter becomes very small the hydrostatic approximation breaks down. As noted by Hoskins (1974), the conservation of q_e in the absence of radiation, dissipation and transfer of heat from the surface implies that these non-conservative processes are necessary to restore an initially unstable atmosphere to stability, unless large-scale downward motion renders the flow unsaturated.

Several precautions must be taken in the applica-

¹ BH derive expressions using the wet bulb potential temperature θ_w rather than the equivalent potential temperature. Following the methods of Durran and Klemp (1982), we find that the square of the moist buoyancy frequency and $f\bar{v}_z$ may be expressed as vertical and horizontal derivatives of $\ln \theta_w$, multiplied by the coefficient

$$g \frac{\Gamma_m(T)}{\Gamma_m(\theta_w)} \left(1 + \frac{L_v q_s}{R\theta_w} \right),$$

where $\Gamma_m(\theta_w)$ is the moist adiabatic lapse rate evaluated at $p = 1000$ mb and $T = \theta_w$, and we have again neglected small effects which depend on the total water content. These expressions differ somewhat from those stated by BH, but it can be shown that the Lagrangian growth rate takes the same simple form as their linear growth rate expression

$$\sigma^2 = -fq_w \left(\frac{\partial \ln \theta_w}{\partial z} \right)^{-1},$$

where q_w is defined as in (29), but with θ_w replacing θ_e .

tion of (31). Since we have assumed saturation in deriving (31), the growth rate thus obtained should be thought of as applying to parcel instability in an atmosphere which is just saturated but contains no liquid water. If, on the other hand, the environment of the slantwise ascending motion is unsaturated, then a positive σ^2 as expressed by (31) should be taken as a necessary but not sufficient condition for instability.

Another problem which occurs in assessing the stability of an entire layer which is lifted to saturation is related to geostrophic adjustment. After a baroclinic layer reaches saturation, ageostrophic motions must occur in order to bring the layer from an unsaturated state of thermal wind balance to the saturated balance described by (30). Such motions must occur in baroclinic flows brought bodily to saturation, whether or not they are unstable to slantwise convection, and may be at least as strong as those resulting from conditional symmetric instability of the layer variety. This renders suspect the assumption of a steady basic state used in describing the instability. This problem does not occur in assessing the stability of isolated masses, rather than entire layers, as they are brought to saturation.

It is evident in Fig. 5 that the mass convergence into the slantwise ascending updraft will generally be associated with a forced convergence of M and θ surfaces near the lower boundary. Qualitatively, one would expect a local frontogenetical circulation to develop as a consequence of this process. The upward motion associated with this circulation will likely be greatest on the warm-air side of the initial slantwise convection. Further investigation of this process is considered beyond the scope of this paper.

3. Discussion

We have examined two cases of moist symmetric instability; the first involves non-hydrostatic motion

in a perfectly moist adiabatic flow while the second is concerned with hydrostatic flow in a fluid which is stable to purely vertical reversible displacements. In fact, the first case is unlikely to be important in the atmosphere, since the hydrostatic approximation will be valid even when the buoyancy frequency is quite small. The hydrostatic approximation applies when the slope of S surfaces is small, the condition for which in a saturated atmosphere may be expressed as

$$N_m^2 \gg f|\bar{v}_z|, \quad (32)$$

where N_m is the saturated buoyancy frequency,

$$N_m^2 \equiv \frac{-g}{\theta_{v0}} \frac{\Delta\theta_v}{\Delta z}.$$

Here $\Delta\theta_v$ is the difference between the virtual potential temperature of a parcel and that of its environment, when the parcel is lifted a small distance Δz . Using this expression, Eq. (32) can be written as

$$\Delta\theta_v \gg \frac{\theta_{v0}}{g} f|\Delta v|,$$

where Δv is a typical change of velocity through a layer. Taking liberal estimates of $\Delta v = 40 \text{ m s}^{-1}$ and $\theta_{v0} = 300 \text{ K}$, we have

$$\Delta\theta_v \gtrsim 0.12 \text{ K}.$$

From this we may conclude that the hydrostatic assumption is applicable very close to the condition of neutral stability. The transition from strongly sloped hydrostatic motions resulting from moist symmetric instability to vertical moist convection will in general be accompanied by only a very brief period of non-hydrostatic symmetric instability.

We next examine the range of conditions under which hydrostatic moist symmetric instability is possible. It is shown in a companion paper (Emanuel, 1983) that in the special case of constant absolute vorticity $\bar{\eta}$ the maximum gravitational and centrifugal potential energy that can be achieved by lifting a tube slantwise in a geostrophic flow is given by

$$\text{PE} = \frac{g}{\theta_{v0}} \int_1^2 \Delta\theta_v dz + \frac{1}{2} \frac{f}{\bar{\eta}} [v_2 - v_1]^2, \quad (33)$$

where points 1 and 2 represent the bottom and top of the layer in question, $\Delta\theta_v$ is the difference between the tube virtual potential temperature and that of its environment, and v_2 and v_1 are the tube-parallel velocity components at the top and bottom of the layer. The first term in (33) is just the area between the applicable adiabat and the environmental temperature on a tephigram, while the second represents the centrifugal potential of a ring of fluid lifted through the layer. A positive value of PE in (33) indicates a potential for instability.

From (33) it can be seen that a velocity difference Δv across a layer is energetically equivalent to a parcel virtual temperature surplus of

$$\Delta\theta_{\text{vin}} \sim \frac{1}{2} \frac{\theta_{v0}}{gH} \frac{f}{\bar{\eta}} (\Delta v)^2,$$

where H is the depth of the layer. If Δv is 40 m s^{-1} across 5 km, the above is equivalent to about 5°C of lifted parcel virtual temperature surplus. This reinforces the suggestion of BH and others that moist symmetric instability should be important in strongly baroclinic moist flows. Examples of potential energy calculations using a more general version of (33) in flows which were observed to contain rainbands are given in Emanuel (1983).

It is interesting to estimate the effects which moist symmetric instability will have on the large-scale flow. The non-hydrostatic calculations suggest that a small amount of heat is transported upward and baroclinically toward the colder air, in good agreement with the linear results of Stone (1972) for dry symmetric instability. Far more certain and quantitatively important are the transports of angular momentum. Since the ascending tubes, until they reach their equilibrium position, always have a smaller amount of angular momentum than their environment, the flow transports angular momentum downward and baroclinically toward the warmer air. The magnitude of the angular momentum transport will of course depend on the mass flux of the ascending flow but the results obtained here suggest that the correlation of angular momentum deficit and flow in the cross-shear direction will be large. The moist symmetric instability, like its dry counterpart, will deplete the momentum of the upper-level jet and deposit it at lower altitudes and baroclinically toward the warmer air.

It should be stressed that the mesoscale horizontal extent and small vertical depth of circulations resulting from moist symmetric instability will not be resolved in most large-scale numerical models; such models may therefore lack an important means by which momentum is transported vertically and horizontally in the atmosphere. Further research on this subject may prove the desirability of incorporating a parameterization of mesoscale transports of momentum by moist symmetric instability.

4. Summary

Simple Lagrangian equations have been developed which describe the slantwise ascent of two-dimensional moist air tubes in convectively stable baroclinic flows, under the assumptions that pressure perturbations are negligible (small Froude number) and mixing is absent. Analytic solutions of these equations for idealized conditions show that the tubes ascend along slantwise paths in such a way that their

buoyancy is nearly zero, although oscillations about this path are possible. In the absence of mixing, the ascending flow reaches equilibrium at the intersection of its surfaces of zero buoyancy and zero angular momentum surplus, and at that intersection reaches maximum velocities which, unless the instability is marginal, are comparable to the velocity of the environmental flow in the tube-parallel direction. These large velocities, together with the implied large aspect ratio of the motion, suggest that turbulent mixing will be important in flows resulting from conditional symmetric instability unless the instability is marginal. In contrast to the assumption of laminar flow, the small Froude number approximation appears to be better justified in this problem than in the case of classical moist convection.

We emphasize the mesoscale character of flow resulting from moist symmetric instability. Shear-parallel rainbands resulting from moist symmetric ascent will have horizontal scales ranging from the same order as the vertical scale, if the flow is close to being moist adiabatic, to as much as two orders of magnitude greater than the vertical scale under conditions of extreme shear. In either case, the small slope of the updraft suggests that water loading will not be a significant inhibition to convection, since precipitation will always fall out of the updraft.

Consideration of the effects of mass convergence into moist slantwise updrafts leads to the expectation that the flow will become more intense on the warm air side of the initial updraft, since the horizontal inflow near the lower boundary will lead to a steepening of surfaces of constant equivalent potential temperature there. Upright moist convection may result if this process continues long enough, as demonstrated by the numerical simulations of BH. A frontogenetical effect is also implied.

Moist symmetric instability, where it is active, may transport significant amounts of momentum. While the angular momentum flux is always down-gradient, the horizontal component of flux appears to be up the horizontal gradient. Large-scale numerical models which do not resolve moist symmetric instability may therefore lack an important means by which momentum is redistributed in the moist baroclinic atmosphere.

It is emphasized that the theory presented here applies to the stability of finite reversible slantwise displacements of a two-dimensional air parcel, or "tube," in an arbitrary baroclinic flow, rather than to infinitesimal displacements in a saturated atmosphere, the stability of which has been previously investigated. In this sense, the present theory is simply an extension of the parcel theory of moist convection which accounts for the centrifugal as well as the gravitational potential energy of a displaced ring of fluid. Unlike the linear theory, the Lagrangian method yields an estimate of the nonlinear characteristics of slantwise convection, including its amplitude. In a companion paper (Emanuel, 1983) we show how the susceptibility of the moist baroclinic atmosphere to local slantwise displacements may be routinely assessed using standard atmosphere soundings.

Acknowledgments. This work was completed with the assistance of Grants ATM-8105012 and ATM-8209375 from the National Science Foundation.

REFERENCES

- Bennetts, D. A., and B. J. Hoskins, 1979: Conditional symmetric instability—a possible explanation for frontal rainbands. *Quart. J. Roy. Meteor. Soc.*, **105**, 945–962.
- Browning, K. A., and T. W. Harrold, 1969: Air motion and precipitation growth in a wave depression. *Quart. J. Roy. Meteor. Soc.*, **95**, 288–309.
- Durrán, D. R., and J. B. Klemp, 1982: On the effects of moisture on the Brunt-Väisälä frequency. *J. Atmos. Sci.*, **39**, 2152–2158.
- Emanuel, K. A., 1979: Inertial instability and mesoscale convective systems. Part I: Linear theory of inertial instability in rotating viscous fluids. *J. Atmos. Sci.*, **36**, 2425–2449.
- , 1982: A variational theorem for circulation integrals applied to inviscid symmetric flows with variable stability and shear. *Quart. J. Roy. Meteor. Soc.*, **108**, 825–832.
- , 1983: On assessing local conditional symmetric instability from atmospheric soundings. *Mon. Wea. Rev.*, **111**, (in press).
- Hoskins, B. J., 1974: The role of potential vorticity in symmetric stability and instability. *Quart. J. Roy. Meteor. Soc.*, **100**, 480–482.
- Houze, R. A., Jr., P. V. Hobbs, K. R. Biswas and W. M. Davis, 1976: Mesoscale rainbands in extratropical cyclones. *Mon. Wea. Rev.*, **104**, 868–878.
- Stone, P. H., 1972: On non-geostrophic baroclinic stability: Part III. The momentum and heat transports. *J. Atmos. Sci.*, **29**, 419–426.